

Deformation of Two Copper Matrix Conductors Under Cyclic Loading

K. Han , V. Toplosky, and C. A. Swenson

Abstract—High field resistive magnets use Cu matrix composites as conductors because composite conductors have high mechanical strength. The conductors are manufactured by cold deformation and heat treatment that introduce refined obstacle distance to resist dislocation motions. The increased density of these obstacles increases the mechanical strength of the conductors. Under cyclic loading, such as the loading condition in pulsed resistive magnets, the conductors may soften or harden depending on the interaction of the obstacles with the dislocations evolved during the loading. Understanding and predicting the performance of the conductors under cyclic loading help researchers to predict the life of the coils made from these conductors, to make efficient use of them in magnets, and to manufacture conductors to meet the requirements of the magnets, particularly when the magnetic stress is above the yield strength of the conductors. The goal of this research is to understand the fatigue properties of two composite conductors and to relate such properties to types of obstacles. The fatigue test loading is in displacement-controlled mode, which is like what occurs in a state-of-the-art pulsed magnet. This work sheds a light on the correlation between the tensile and fatigue properties in composite conductors by consideration of types of obstacle in composite conductors.

Index Terms—Alloy, deformation, high strength steels, high field magnet, reinforcement.

I. INTRODUCTION

THE term “Cu matrix conductor” is used in this article to refer to any material that contains Cu as either the matrix or one of the major elements. When these conductors are comprised of two or more dissimilar phases to produce composite, these phases can work synergistically to produce properties that are better than rule-of-mixture [1]. This paper is focused on metal-metal composite conductors, in which both the matrix and the second phase are ductile metals. These composites have attracted attention for their blending of ultra-high strength with good electrical and thermal conductivity. They have potential applications in several fields where tensile strength greater than

Manuscript received November 30, 2021; revised February 20, 2022 and March 7, 2022; accepted March 14, 2022. Date of publication April 14, 2022; date of current version May 2, 2022. The work was undertaken in the National High Magnetic Field Laboratory, which is supported by National Science Foundation DMR-1644779 and the State of Florida. (Corresponding author: K. Han.)

K. Han and V. Toplosky are with National High Magnetic Field Laboratory, Tallahassee FL32310 USA (e-mail: hanke666666@hotmail.com; toplosky@magnet.fsu.edu).

C. A. Swenson is with the Lawrence Berkeley National Laboratory, Berkeley, CA 94720-8203 USA (e-mail: caswenson@lbl.gov).

Color versions of one or more figures in this article are available at <https://doi.org/10.1109/TASC.2022.3166712>.

Digital Object Identifier 10.1109/TASC.2022.3166712

0.5 GPa and electrical conductivity above 60% IACS (International Annealed Copper Standard) are required, such as windings of high-field magnet cables.

In general, Cu-base composites are represented as Cu-X-Y ..., with X-Y ... representing such elements as Ag, Cr, Fe, Mo, Nb, Ti, V, or Zr. These materials can be further classified by their strengthening component: Cu-fcc (face-centered cubic), Cu-bcc (body-centered cubic), or Cu-IM (intermetallic compounds).

For production of composites, the *in-situ* method is an inexpensive way to produce large size products. A composite is referred to as *in-situ* when the composite structure has been formed during solidification or heat [2]–[11]. With proper control of solidification rates and/or heat treatment temperature/time, this composite structure will be a refined microstructure that can then be further refined by heavy deformation through sheet rolling and wire swaging/ drawing. Additional strain can be imparted to the material via re-bundling followed by further deformation of already heavily deformed wires [1]. Since both metallic phases of a metal-metal nanocomposite are ductile, it is possible to achieve true strain values greater than ten (or 1000%). By selection of chemistry and fabrication methods, the second phase can be made into the fiber or particle shapes. We believe that deformation behavior is drastically different from one type to the other with important implications for service life in magnet coils. We therefore studied deformation behavior of Cu-Ag-Zr (fibers) and Cu-Ag-Cr (particle) Cu-matrix *in-situ* composites by close examination of their stress-strain curves for tension and cyclic loading.

II. METHODS

A. Materials

The conductor wires were made of either Cu-Ag(Zr) or Cu-Ag-Cr. The materials were received in a dimension of 4x6 mm² form. The Cu-Ag(Zr) was custom-made for this study to a higher standard of mechanical strength than is commercially available [12]–[15]. Cu-Ag(Zr) can be considered as Cu-fcc-IM, where fcc phase took the form of Ag fibers and IM took the form of particle containing Zr. Because the numbers of IM were small, we refer this material as CuAg in this manuscript. In this composite, Ag and Cu usually has cube-on-cube relationship [16]. The Cu-Ag-Cr (Wieland K-88) was made by Wieland to the European commercial standard, which is similar to the 18200/18400/18500 American standard (see Table I). The strengthening component was either fcc or bcc Cr phase, where bcc Cr had an N–W relationship with the matrix. Because

TABLE I
CHEMISTRY OF THE ALLOYS (WT%)

Elements	Cr	Ag	Fe	Ti	Si	Zr	Cu
CuAg		7				0.05	Bal-
CuCr	0.5	0.1	0.08	0.06	0.03	0.38	ance

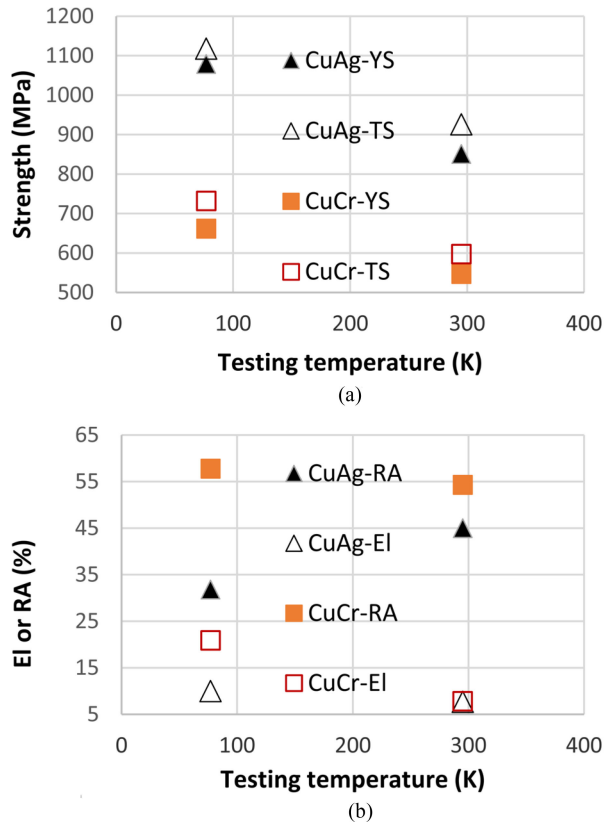


Fig. 1. Tensile properties for reduced-cross-section samples. These data are from tensile testing of cold-deformed CuAg and CuCr samples. Tests were performed at either 295 K or 77 K. Data for samples are taken from either CuCr wire, indicated by squares, or CuAg wire, indicated by triangles. (a) Yield Strength (YS) values are shown by solid triangles or squares. Ultimate Tensile Strength (TS) values are shown by open triangles or squares. (b) The values of Reduction in Area at fracture (RA) are shown by solid triangles or squares. Elongation (EL) is shown by open triangles or squares.

Ag content was low, we refer this material as CuCr in this manuscript.

B. Tensile Property Characterization

Most mechanical tests were performed at 295 K and 77 K, per ASTM E8-00b and ASTM A370-97a. In tensile tests, the samples were machined to a gage cross-section of $3 \times 4 \text{ mm}^2$. The samples were loaded in displacement control mode at a rate of 0.5 mm/min on a 100 kN servo-hydraulic MTS test machine. From the measured stress-strain curves, both ultimate tensile strength (TS) and 0.2% offset engineering flow stress (YS = Yield Strength) were recorded (Fig. 1).

We used reduced cross-section samples to reduce the stress-concentration introduced by grips. At both room and cryogenic

temperatures, our experiments showed that samples from reduced cross-section samples showed higher mechanical strength than that from full cross-section samples.

C. Fatigue Tests

Reverse cycle fatigue tests were performed with the same machine and test temperatures as tensile tests. Testing was performed in a displacement control mode via a diametral displacement gauge until failure. Testing frequency was 5 Hz.

D. Electrical Conductivity Tests

For conductivity measurements, voltage taps were mechanically clamped on the specimens at approximately 100 mm apart. Current leads are attached to the ends of the specimens and input currents of 0.25, 0.50, 0.75, and 1.0 amps are used to obtain the voltage drop across the voltage tap distance. Three samples were measured, and the value reported here is the average of the three measurements and is estimated to be accurate within $\pm 1\%$ IACS.

III. RESULTS

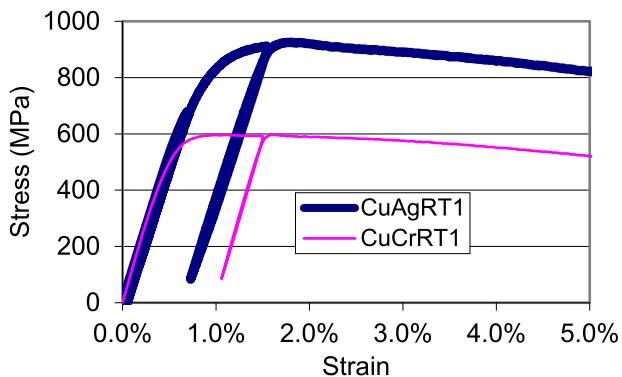
A. Tensile Properties and Electrical Conductivity

Tensile tests performed at cryogenic and room temperatures showed a range of variation in both ultimate Tensile Strength (TS) and Yield Strength (YS). Property differences within the same materials tested under the same condition, however, were minor. At 77 K, variation in the value of TS was 0.6% for CuAg and 0.4% for CuCr. The maximum variation in the value of YS was about 3% for both. This indicates that both conductors are homogeneous.

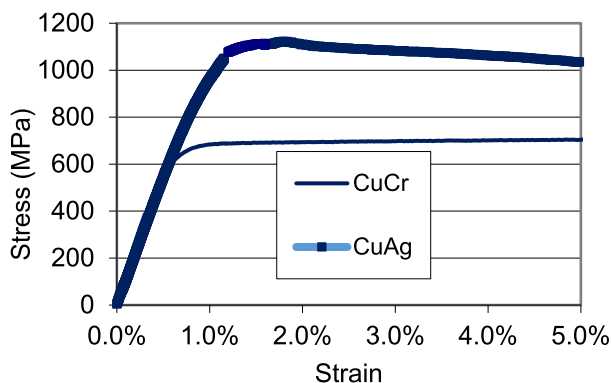
We used both TS and YS to compare properties from CuAg and CuCr samples. At both cryogenic and room temperatures, tests showed higher mechanical strength in CuAg than in CuCr (Fig. 1). At room temperature, for example, the value of TS for CuAg was 55% higher than for CuCr. At 77 K, the value of TS for CuAg was 53% higher than for CuCr. Variation between samples of different materials was much greater than variation between samples of the same material, thus indicating that the difference between the tensile properties of these two materials could not be dismissed as experimental error. We attributed it rather to the difference in the chemistry and geometry of the strengthening components of the two materials. Although both materials were made by drawing and aging cast ingots, the CuAg was strengthened by Ag in the form of fibers while the CuCr was strengthened by Cr in the form of particles [16]–[38]. As both materials have the same Cu matrix, our result indicates that fibers strengthen wire more effectively than particles.

Both materials showed more than 20% higher tensile strength at 77 K than at room temperature and they had a higher modulus (12% higher for Cu-Ag and 3% higher for Cu-Cr). This may reflect an improvement at cryogenic temperature in their ability to withstand further plastic deformation after their initial elastic deformation.

To estimate strain-hardening rates, we calculated the ratio between TS and YS in both materials. We found that the values



(a)



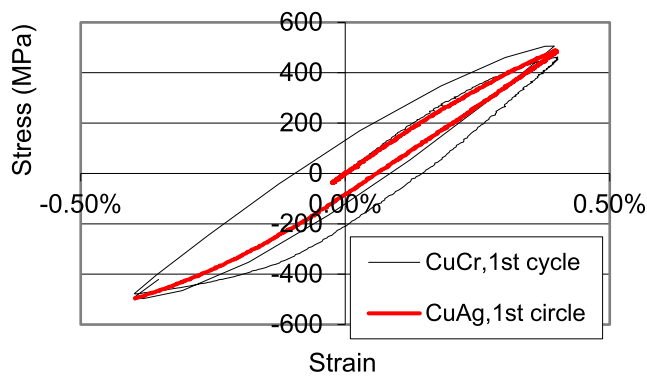
(b)

Fig. 2. Stress-strain curves of CuCr (thin line) and CuAg (thick line). Tests were performed: (a) at room temperature and (b) at 77 K.

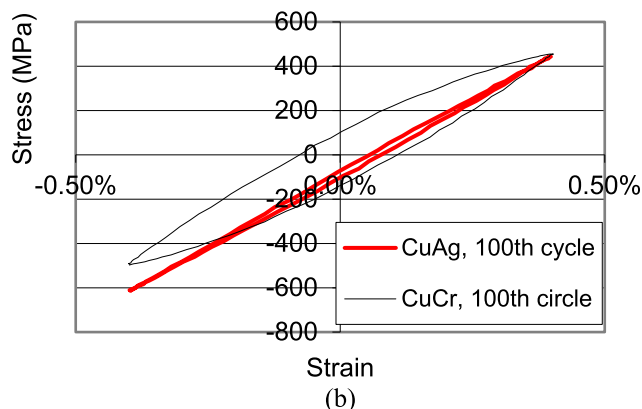
of TS/YS for CuAg were 1.09 at room temperature and 1.04 at 77 °K, and for CuCr 1.09 at room temperature and 1.11 at 77 °K. The greater value of TS/YS for CuCr at 77 °K clearly indicated that CuCr could be further hardened by deformation. Despite the fact that CuAg already had very high tensile strength, these TS/YS ratios indicated that it too could be hardened even further by deformation. We noticed that CuAg samples had higher TS/YS values at room temperature than at 77 °K, while CuCr samples had higher TS/YS values at 77 °K than at room temperature (Fig. 1). This may indicate that, during room temperature deformation, dynamic recovery plays a bigger part in CuCr than in CuAg. In other words, cryogenic temperature tends to suppress dynamic recovery in CuCr more than in CuAg (Fig. 2).

Values for elongation-to-failure (EL) were all above 7%, and values for reduction-in-area-at-fracture (RA) were all above 30% in both materials at both temperatures. The value of EL at room temperature, which was similar for the two materials, was 7%, the lowest among all the ductility values. Our previous experiments indicated that this value was sufficient for conductors to reach bending strain above 40%. At this strain, a 4-mm-thick wire can be wound in a coil with a diameter smaller than 10 mm.

At 77 °K, both EL and RA values increased for Cu-Cr, less in RA than in EL. We attributed this increase mainly to the



(a)



(b)

Fig. 3. Stress-strain curves of Cu-Cr (thin line) and Cu-Ag (thick line) under cyclic loading with total strain amplitude of 0.8%. Tests were performed under symmetric displacement control mode at room temperature. (a) Comparison of the curves at first cycle. (b) Comparison of the curves at 100th cycle.

larger homogeneous deformation strain that resulted from the enhanced strain hardening that occurred because of suppressed dynamic recovery or recrystallization at cryogenic temperatures (Fig. 2). At 77 °K, Cu-Ag showed good ductility before the onset of instability, although it showed certain softening after yielding. After the onset of instability, however, Cu-Ag showed higher EL but lower RA than at room temperature, indicating some loss of ductility. Cu-Ag showed higher electrical conductivity at 77 K than Cu-Cr (Fig. 5)

B. Cyclic Loading Properties

Reinforcement materials are used in most of the high-field pulsed magnets in our laboratory because reinforcement limits the displacement that occurs in those conductors. Consequently, we chose to apply the displacement-controlled mode when we performed our cyclic tests.

At room temperatures, once strain exceeded the relevant elastic strain limit, different plastic deformation behavior appeared in each of the two materials tested. This was consistent with the results of tensile tests. (For an example of this behavior difference between two samples under cyclic loading of a total strain amplitude (ϵ_t) of 0.8%, see Fig. 3). During the first cycle of loading, the Cu-Ag samples, whose YS was higher, showed a higher stress level and less plastic deformation strain (ϵ_p) than

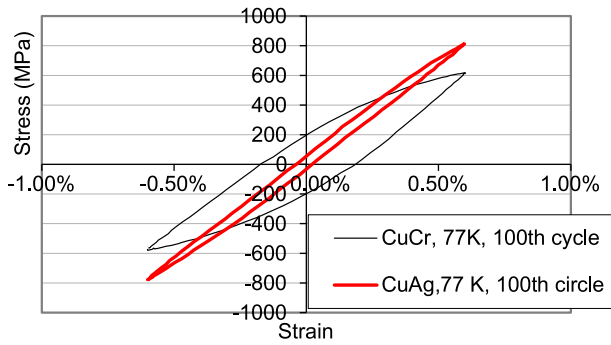


Fig. 4. Stress-strain curves of Cu-Cr (thin line) and Cu-Ag (thick line) under cyclic loading with total strain amplitude of 1.2%. Tests were performed under symmetric displacement control mode at 77 °K.

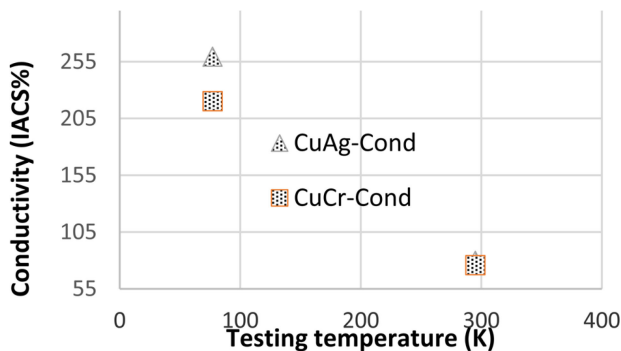


Fig. 5. Electrical conductivity of CuAg and CuCr samples. Tests are performed at either 295 °K or 77 °K. Data for CuAg and CuCr samples are indicated by triangles and squares, respectively.

Cu-Cr samples under the same e_t . In this first cycle, tensile stress levels (s_t) were almost the same as the absolute value of compressive stress levels ($-s_c$) for both materials, indicating that they responded symmetrically to tensile and compressive loads (Fig. 3). When both materials were loaded to cycle 100, the values of s_t were smaller than those of $-s_c$. Cu-Ag showed almost the same s_t level as Cu-Cr but had a higher $-s_c$ under the same e_t . Cu-Ag continued to show significantly less plastic deformation strain (e_p) than Cu-Cr. As a result, Cu-Ag samples outlasted those of Cu-Cr, even though the Cu-Ag was subjected to higher stress amplitude (Fig. 6).

Because both materials showed higher YS at 77 °K, we loaded the materials to a greater e_p at 77 °K than at room temperature in order to study their plastic deformation behaviors. At 77 °K, plastic deformation began as soon as strain exceeded the elastic strain limit. This was similar to what we observed in room temperatures. (For an example of this behavior difference between two samples under cyclic loading of an e_t of 1.2%, see Fig. 4). During the first cycle of loading at 77 °K, the materials showed plastic deformation behavior similar to that at room temperature. When both materials were loaded to cycle 100, the values of s_t remained almost the same as those of $-s_c$. At the same e_p level, Cu-Ag showed higher stress levels than Cu-Cr.

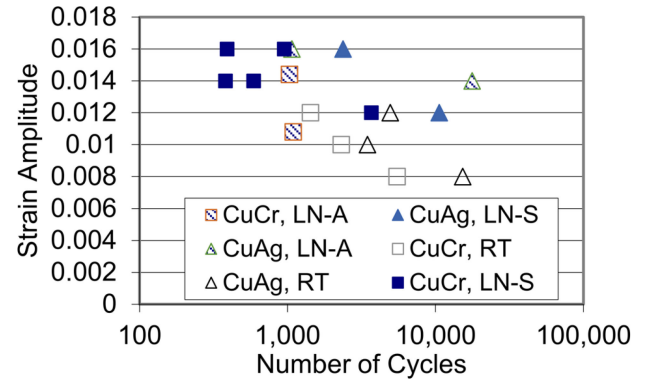


Fig. 6. Strain amplitude with respect to the number of cycles to failure. Data taken from CuAg samples are indicated by open or solid triangles, from CuCr samples by open or solid squares. Room temperature data indicated by open triangles or squares; data obtained at 77 °K under symmetric strain are indicated by solid triangles or squares; that obtained under asymmetric strain, by shaded triangles or squares.

Even so, Cu-Ag continued to show less plastic deformation strain (e_p) than Cu-Cr (Fig. 4). The smaller value of e_p in Cu-Ag led to longer service life (Fig. 6).

IV. DISCUSSION

In this study, fiber-strengthened Cu showed higher mechanical strength than particle strengthened Cu. Both types of materials showed higher mechanical strength at cryogenic temperatures because of the suppression of dynamic recovery. When the two materials were subjected to the same total strain amplitude at both room and cryogenic temperatures, fiber-strengthened Cu showed longer fatigue life, even though the fiber-strengthened Cu had been forced by its higher strain-hardening rate to reach higher stress levels. This longer fatigue life was attributed to the fact that less plastic deformation strain occurred in fiber-strengthened Cu because its fine fiber spacing reduced the travel distance of dislocations in comparison to particle-strengthened Cu.

V. CONCLUSION

Cu-Ag samples that were strengthened by fibers had higher strength but lower ductility than Cu-Cr samples that were strengthened by particles. At same total strain amplitude, Cu-Ag reached higher strength but experienced lower plastic deformation strain at both room and cryogenic temperatures. The lower level of plastic deformation in Cu-Ag led to a longer fatigue life in comparison to Cu-Cr.

ACKNOWLEDGMENT

The authors would like to thank S. Zherlitsyn, J. Freudenberger, A. Gaganova, and D. N. Nguyen for discussion and providing samples and M. Tyler for editing.

REFERENCES

- [1] K. Han *et al.*, "The fabrication, properties and microstructure of Cu–Ag and Cu–Nb composite conductors," *Mater. Sci. Eng.: A*, vol. 267, no. 1, pp. 99–114, 1999.
- [2] J. D. Embury, K. Han, J. R. Sims, V. I. Patsyrnyi, and A. Shikov, "Fabrication routes for high strength-high conductivity wires," in *VIIIth Int. Conf. Megagauss Magn. Field Generat. Relat. Top.*, H. Schneider-Muntau ed., World Scientific, MGVIII, 2004, pp. 158–160.
- [3] K. Han, J. P. Hirth, and J. D. Embury, "Modeling the formation of twins and stacking faults in the Ag–Cu system," *Acta Materialia*, vol. 49, no. 9, pp. 1537–1540, May 2001.
- [4] K. Han *et al.*, "High strength conductors and structural materials for high field magnets," *MRS Adv.*, vol. 1, no. 17, pp. 1233–1239, 2016.
- [5] K. Han, V. J. Toplosky, R. Goddard, J. Lu, R. Niu, and J. Chen, "Impacts of heat treatment on properties and microstructure of Cu16at% Ag conductors," *IEEE Trans. Appl. Supercond.*, vol. 22, no. 3, Jun. 2012, Art. no. 6900204.
- [6] G. M. Li *et al.*, "Influence of high magnetic field on as-cast structure of Cu-25wt% Ag alloys," *China Foundry*, vol. 10, no. 3, pp. 162–166, May 2013.
- [7] C. C. Zhao *et al.*, "Strength of Cu-28 wt%Ag composite solidified under high magnetic field followed by cold drawing," *Met. Mater. Int.*, vol. 23, no. 2, pp. 369–377, Mar. 2017.
- [8] C. C. Zhao *et al.*, "Simultaneously increasing strength and electrical conductivity in nanostructured Cu–Ag composite," *Mater. Sci. Eng. A-Struct. Mater. Properties Microstructure Process.*, vol. 652, pp. 296–304, Jan. 2016.
- [9] X. W. Zuo *et al.*, "Microstructure and properties of Cu-6wt% Ag composite thermomechanical-processed after directionally solidifying with magnetic field," *J. Alloys Compounds*, vol. 676, pp. 46–53, Aug. 2016.
- [10] X. W. Zuo *et al.*, "Microstructure and properties of nanostructured Cu28 wt%Ag microcomposite deformed after solidifying under a high magnetic field," *Mater. Sci. Eng. A-Struct. Mater. Properties Microstructure Process.*, vol. 619, pp. 319–327, Dec. 2014.
- [11] X. W. Zuo *et al.*, "Precipitation and dissolution of Ag in ageing hypoeutectic alloys," *J. Alloys Compounds*, vol. 622, pp. 69–72, Feb. 2015.
- [12] A. Gaganov *et al.*, "Effect of Zr additions on the microstructure, and the mechanical and electrical properties of Cu-7 wt.%Ag alloys," *Mater. Sci. Eng. A-Struct. Mater. Properties Microstructure Process.*, vol. 437, no. 2, pp. 313–322, Nov. 2006.
- [13] A. Gaganov *et al.*, "Microstructural evolution and its effect on the mechanical properties of Cu–Ag microcomposites," *Zeitschrift Fur Metallkunde*, vol. 95, no. 6, pp. 425–432, Jun. 2004.
- [14] S. Spaic and M. Pristavec, "Precipitation on hardening behaviour in Cu–Ag alloys with additions of zirconium," *Metall*, vol. 50, no. 4, pp. 254–256, Apr. 1996.
- [15] Y. H. Zhou, H. H. Zhao, and K. H. Zhang, "Investigation of the Ag–Cu–Zr ternary-system," *J. Less-Common Met.*, vol. 138, no. 1, pp. 7–10, Mar. 1988.
- [16] K. Han *et al.*, "Microstructural aspects of Cu–Ag produced by the Taylor wire method," *Acta Materialia*, vol. 46, no. 13, pp. 4691–4699, Aug. 1998.
- [17] D. Raabe *et al.*, "Metallic composites processed via extreme deformation: Toward the limits of strength in bulk materials," *MRS Bull.*, vol. 35, no. 12, pp. 982–991, Dec. 2010.
- [18] S. Tardieu *et al.*, "Nanostructured 1% silver-copper composite wires with a high tensile strength and a high electrical conductivity," *Mater. Sci. Eng. A-Struct. Mater. Properties Microstructure Process.*, vol. 761, Jul. 2019, Art. no. 138048.
- [19] S. Tardieu *et al.*, "High strength-high conductivity silver nanowire-copper composite wires by spark plasma sintering and wire-drawing for non-destructive pulsed fields," *IEEE Trans. Appl. Supercond.*, vol. 30, no. 4, Jun. 2020, Art. no. 6900304.
- [20] S. Tardieu *et al.*, "Influence of alloying on the tensile strength and electrical resistivity of silver nanowire: Copper composites macroscopic wires," *J. Mater. Sci.*, vol. 56, no. 7, pp. 4884–4895, Mar. 2021.
- [21] K. Han *et al.*, "Material issues in the 100 T non-destructive magnet," *IEEE Trans. Appl. Supercond.*, vol. 10, no. 1, pp. 1277–1280, Mar. 2000.
- [22] K. Han *et al.*, "The fabrication, properties and microstructure of Cu–Ag and Cu–Nb composite conductors," *Mater. Sci. Eng. A-Struct. Mater. Properties Microstructure Process.*, vol. 267, no. 1, pp. 99–114, Jul. 1999.
- [23] K. Han *et al.*, "Internal stresses in cold-deformed Cu–Ag and Cu–Nb wires," *Philos. Mag.*, vol. 84, no. 24, pp. 2579–2593, Aug. 2004.
- [24] K. Han, V. J. Toplosky, R. Walsh, C. Swenson, B. Lesch, and V. I. Patsyrnyi, "Properties of high strength Cu–Nb conductor for pulsed magnet applications," *IEEE Trans. Appl. Supercond.*, vol. 12, no. 1, pp. 1176–1180, Mar. 2002.
- [25] K. Han, V. J. Toplosky, Y. Xin, J. R. Sims, and C. A. Swenson, "Fatigue property examinations of conductors for pulsed magnets," *IEEE Trans. Appl. Supercond.*, vol. 20, no. 3, pp. 1463–1466, Jun. 2010.
- [26] D. W. Yuan *et al.*, "Upward continuous casting in the manufacture of Cu–Cr–Ag alloys: Potential for enhancing strength whilst maintaining ductility," *Metallurgical Mater. Trans. A-Phys. Metall. Mater. Sci.*, vol. 48A, no. 12, pp. 6083–6090, Dec. 2017.
- [27] S. Xu *et al.*, "Effect of Ag addition on the microstructure and mechanical properties of Cu–Cr alloy," *Mater. Sci. Eng. A-Struct. Mater. Properties Microstructure Process.*, vol. 726, pp. 208–214, May 2018.
- [28] G. L. Xu *et al.*, "Microstructural evolution and properties of a Cu–Cr–Ag alloy during continuous manufacturing process," *Rare Met.*, vol. 40, no. 8, pp. 2213–2220, Aug. 2021.
- [29] C. Watanabe, R. Monzen, and K. Tazaki, "Mechanical properties of Cu–Cr system alloys with and without Zr and Ag," *J. Mater. Sci.*, vol. 43, no. 3, pp. 813–819, Feb. 2008.
- [30] Y. Q. Sun *et al.*, "Effect of Ag on properties, microstructure, and thermostability of Cu–Cr alloy," *Materials*, vol. 13, no. 23, Dec. 2020, Art. no. 11.
- [31] J. Seeger *et al.*, "K88/C18080—A customer designed alloy for connector application," *Metall*, vol. 56, no. 5, pp. 289–292, 2002.
- [32] D. Raabe, K. Miyake, and H. Takahara, "Processing, microstructure, and properties of ternary high-strength Cu–Cr–Ag in situ composites," *Mater. Sci. Eng. A-Struct. Mater. Properties Microstructure Process.*, vol. 291, no. 1/2, pp. 186–197, Oct. 2000.
- [33] D. Raabe and J. Ge, "Experimental study on the thermal stability of Cr filaments in a Cu–Cr–Ag in situ composite," *Scripta Materialia*, vol. 51, no. 9, pp. 915–920, Nov. 2004.
- [34] K. M. Liu *et al.*, "Microstructure and properties of Cu–Cr–Ag in-situ composites," *Rare Metal Mater. Eng.*, vol. 40, no. 11, pp. 1931–1935, Nov. 2011.
- [35] D. Liang *et al.*, "Relationship between microstructure and properties of Cu–Cr–Ag alloy," *Materials*, vol. 13, no. 3, Feb. 2020, Art. no. 8.
- [36] M. Keppeler *et al.*, "New copper materials for electronics and electrical engineering," *Metall*, vol. 57, no. 7/8, pp. 460–465, 2003.
- [37] R. K. Islimgaliev *et al.*, "Structure and crystallographic texture in the Cu–Cr–Ag alloy subjected to severe plastic deformation," *Rev. Adv. Mater. Sci.*, vol. 39, no. 1, pp. 61–68, Dec. 2014.
- [38] H. M. Chen *et al.*, "Relationship between microstructure and properties of Cu–Cr–Ag–(Ce) alloy using microscopic investigation," *Scanning*, 2017, Art. no. 4646581.